Delft University of Technology

Optimization Strategy for Flexible Operation of Integrated Multi-Energy Industrial Clusters

Zuijderwijk, Iza Rian; Torres, José Luis Rueda; Palensky, Peter

Optimization Strategy for Flexible Operation of Integrated Multi-Energy Industrial Clusters

Iza Rian Zuijderwijk, José Luis Rueda Torres, Peter Palensky

Department of Electrical Sustainable Energy
Delft University of Technology
Delft, The Netherlands
(I.R.Zuijderwijk, J.L.RuedaTorres, P.Palensky)@tudelft.nl

Abstract—Achieving carbon neutrality in industrial ports demands a radical transformation of current energy systems. This paper presents a model-based optimization approach for the operation of a multi-energy cluster, considering a hypothetical evolution of a multi-energy industrial cluster in the Netherlands. The aim is to establish a new system operation strategy that supports the transition towards a carbon-neutral energy system. The synthetic model of the used multi-energy cluster integrates five energy carriers—electricity, natural gas, hydrogen, ammonia, and heat—using an energy hub approach to enable sector coupling and enhance flexibility. Physics-based modeling of electrical power flows is included to ensure technical feasibility in the power system. The model minimizes total cluster's cost while ensuring reliable energy supply. The optimization is implemented in Python by using the PyPSA toolbox and mixed-integer linear programming. A full-year, hourly-resolution simulation under three weather scenarios reveals optimal system operation strategies. Numerical results highlight the benefits of multi-energy cluster operation for managing renewable variability and identify ammonia as a key flexibility provider, supporting hydrogen and electricity systems through conversion and storage. The strategy emphasizes cross-sector economic optimization, dynamic dispatch, and enhanced flexibility, offering practical insights for decarbonizing industrial ports and informing future energy investment planning.

Index Terms—Multi-energy system, sector coupling, flexibility, system operation

I. INTRODUCTION

The Netherlands faces an urgent need to reduce its greenhouse gas emissions, with national targets aiming for a 55% reduction by 2030 and carbon neutrality by 2050. An industrial cluster could theoretically be responsible for nearly 17% of national CO_2 emissions, playing an important role in achieving these targets. However, the transition towards a carbon-neutral port is hindered by several challenges. The increasing integration of variable renewable energy sources (VRES) introduces intermittent energy production, straining power infrastructure and system balancing capabilities. At the same time, industrial electrification drives a substantial increase in electricity demand, further intensifying pressure on the power system. Grid congestion remains a major issue

despite ongoing reinforcement efforts, threatening energy supply reliability—a critical factor for maintaining an attractive investment climate. Development of new energy infrastructure is hindered by limited grid capacity, investment uncertainty, and spatial constraints. Traditional energy systems, structured around decoupled energy sectors, lack the flexibility and coordination needed to address these challenges [1]. Multi-energy systems (MESs) offer a solution by integrating and optimizing multiple energy carriers into a unified operational framework. MESs enable sector coupling, conversion, and storage, allowing energy to flow dynamically across carriers. This enhances the system's ability to decarbonize the energy sector and effectively integrate VRES, while maximizing the use of existing grid infrastructure [2]. While the concept of MES is well-established, operational strategies for future systems that include emerging carriers like hydrogen and ammonia remain underexplored. This paper proposes a novel model-based approach to MES modeling and introduces a new system operation strategy, optimizing its operation under various weather scenarios.

II. LITERATURE REVIEW AND RESEARCH CONTRIBUTION

Most operational MES studies focus on conventional carriers (electricity, gas, heat), with limited attention to alternative carriers such as hydrogen, methane, and ammonia. Hydrogen is typically modeled with a single function—either for storage, syngas production, or ammonia synthesis [3]–[8]. Only a few studies, such as Koirala et al. [9], explore combined roles, yet direct industrial use is largely absent. Ammonia is even less integrated, often confined to storage or power generation applications [6], [8], [10]. Moreover, the common use of energy hub models in MES studies often oversimplifies physical network behavior. A study by Wang and Shao [11] incorporates physics-based modeling of both electricity and gas flows, but excludes alternative energy carriers, limiting applicability to future systems. Heat networks are also typically modeled without temperature differentiation, leading to an incomplete representation of thermal integration.

Contributions of this study to the existing literature:
- Integrating ammonia as a multifunctional energy carrier
- Exploring hydrogen's diverse roles
- Integrating physical power flow into the energy hub approach

- Incorporating temperature-differentiated heat flows
- Providing actionable guidance on system operation strategies and design, beyond purely methodological modeling

III. PROPOSED APPROACH

The study considers a hypothetical evolution of a multi-energy industrial cluster in the Netherlands. The conceptual MES model was developed to represent existing infrastructure, planned projects, and potential future expansions. The system integrates five energy carriers: electricity, natural gas, hydrogen, ammonia, and heat.

A. System Description

Fig. 1 shows a schematic representation of a synthetic (model data and parameters inspired from literature) multi-energy industrial cluster.
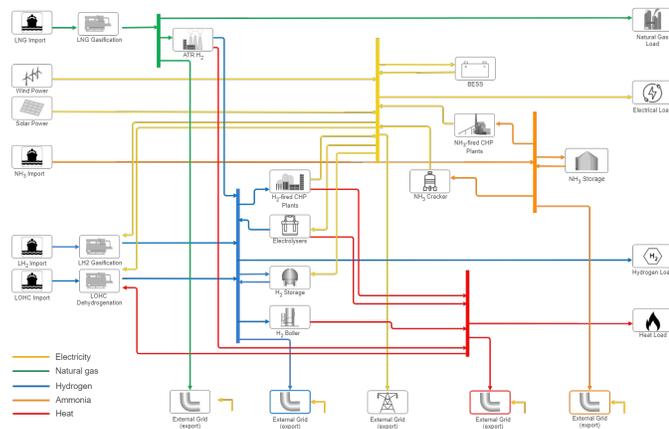

Fig. 1. Schematic Representation of the synthetic multi-energy cluster.

The system includes:

1) Generation and Import: wind farms (Hollandse Kust Zuid, Maasvlakte 2, IJmuiden Ver, Nederwiek), solar farm (De Slufter), and imports of LNG, LH_2, LOHC, and ammonia.
2) Demand: industrial consumers categorized into bio-refineries, chemical industry, terminals, CCUS, and shore power, with hydrogen replacing natural gas for high-temperature heat processes.
3) Conversion: CHP plants (ammonia-fired and hydrogen-fired), hydrogen production (electrolyzers, ATR, ammonia crackers), and import conversion (LNG/LH_2 gasification, LOHC dehydrogenation).
4) Storage: battery energy storage, underground hydrogen storage, hydrogen pressurized tank storage, and ammonia refrigerated tank storage.
5) Transmission and Distribution: the electricity network is modeled using its existing AC topology, while pipelines for gas, hydrogen, ammonia, and heat are represented in aggregated form. Heat network is represented by a district heating network with a 120°C supply side and a 70°C return side.

6) External networks: exports include electricity to the Dutch power grid, natural gas to the national gas network, hydrogen to hinterland industries, ammonia for local applications within the port, and heat to the WarmtelinQ district heating network.

The model includes CCUS technologies, assuming full CO_2 capture and storage and thus carbon neutrality.

B. Modeling Approach

The optimization model was developed using the PyPSA toolbox in Python, selected for its ability to model electrical networks in detail [12]. To verify its reliability, PyPSA was benchmarked against the validated IEEE 9-bus system in PandaPower. Power flow results showed close agreement, confirming PyPSA's suitability for accurate power system modeling in this study.

TABLE I
OVERVIEW OF MODELING ASPECTS USED IN THE MES.

Aspect	Details
Time horizon	Short-term horizon with a one-year simulation
Time resolution	Hourly intervals
Spatial coverage and resolution	Multi-node system covering the industrial cluster area
Sectoral coverage	Energy sectors: electricity, natural gas, hydrogen, ammonia, and heat Demand sectors: industry (consumers located in the industrial cluster)
Methodological approach	Single-objective dispatch optimization with storage capacity optimization
Level of detail	Grey-box; energy-hub approach with physic-based power flow modeling
Assessment criteria	Economic
Programming technique	Mixed-Integer Linear Programming (MILP)
Uncertainty of data	Deterministic approach with scenario analysis

C. Model Formulation

This section will delve into the mathematical formulations of the objective function, decision variables, and constraints.

1) Decision variables: An overview of the input variables for the optimization model is shown in Table II. The decision variables are shown in Table III.

2) Objective function: The objective function, presented is defined as the minimization of the total system's cost:

$$\min_{\substack{\bar{g}_{n,s}, F_l, \bar{h}_{n,s}, \\ g_{n,s,t}, f_{l,t}, h_{n,s,t},}} \left\{ \sum_{n,s} c_{n,s}\bar{g}_{n,s} + \sum_l c_l F_l + \sum_{n,s} c_{n,s}\bar{h}_{n,s} \right.$$
$$\left. + \sum_t w_t \left[\sum_{n,s} o_{n,s,t}g_{n,s,t} + \sum_l o_{l,t}f_{l,t} + \sum_{n,s} o_{n,s,t}h_{n,s,t} \right] \right\} \quad (1)$$

3) Constraints: The constraints define the allowable values of the decision variables and reflect the technical and physical limitations of the system components.

a) Generator constraints: Generators with time-dependent restrictions on the dispatch are constrained by their availability:

$$\tilde{g}_{n,s,t} \cdot \bar{g}_{n,s} \leq g_{n,s,t} \leq \bar{g}_{n,s,t} \cdot \bar{g}_{n,s} \quad (2)$$

For generators that allow curtailment of their energy output, unit commitment can be enabled or disabled:

$$u_{n,s,t} \cdot \tilde{g}_{n,s,t} \cdot \bar{g}_{n,s} \leq g_{n,s,t} \leq u_{n,s,t} \cdot \bar{g}_{n,s,t} \cdot \bar{g}_{n,s} \quad \forall n, s, t \quad (3)$$

Generators whose rated power can be extended in optimization are constrained to:

$$\tilde{g}_{n,s} \leq \bar{g}_{n,s} \leq \hat{g}_{n,s} \quad (4)$$

TABLE II
INPUT VARIABLES

Input Variable	Description
$n \in N = \{0, \ldots, \|N\| - 1\}$	Set of network busses
$t \in T = \{0, \ldots, \|T\| - 1\}$	Set of network snapshots
$l \in L = \{0, \ldots, \|L\| - 1\}$	Set of network branches
$s \in S = \{0, \ldots, \|S\| - 1\}$	Set of generator and/or storage types at each bus
$\bar{g}_{n,s}$	Nominal power of generator
$\bar{e}_{n,s}$	Nominal energy of store
F_l	Nominal capacity of branch l (i.e. link, line, or transformer)
$d_{n,s,t}$	Capacity of load d at time t
$\tilde{g}_{n,s}$	Min. nominal power of generator, if $\bar{g}_{n,s}$ is extendable
$\hat{g}_{n,s}$	Max. nominal power of generator, if $\bar{g}_{n,s}$ is extendable
$\tilde{e}_{n,s}$	Min. nominal energy of store, if $\bar{e}_{n,s}$ is extendable
$\hat{e}_{n,s}$	Max. nominal energy of store, if $\bar{e}_{n,s}$ is extendable
$\tilde{f}_l$	Min. nominal power of branch, if $d_{n,s,t}$ is extendable
$\hat{f}_l$	Max. nominal power of branch, if $d_{n,s,t}$ is extendable
$\tilde{g}_{n,s,t}$	Lower limit of time-dependent restriction of generator
$\bar{g}_{n,s,t}$	Upper limit of time-dependent restriction of generator
$\tilde{f}_{l,t}$	Lower limit of time-dependent restriction of branch
$\bar{f}_{l,t}$	Upper limit of time-dependent restriction of generator
$u_{n,s,t}$	Binary value for unit commitment
rd_l	Ramp-up limit up of link l
ru_l	Ramp-down limit of link l
$\eta_{n,s}$	Efficiency of generator g
η_l	Efficiency of branch l
$\eta_{\text{stand},n,s}$	Standing efficiency of store e
$c_{n,s}$	Capital cost of increasing nominal power by 1 MW
c_l	Capital cost of increasing branch capacity by 1 MW
$o_{n,s}$	Marginal cost of increasing dispatch by 1MWh
o_l	Marginal cost of increasing branch's (link) dispatch by 1MWh
w_t	Weighting of time, equals 1 in hourly simulation

TABLE III
DECISION VARIABLES

Decision variable	Description
$g_{n,s,t}$	Power output of generator s at bus n at time t
$h_{n,s,t}$	Power output of store s at bus n at time t
$f_{l,t}$	Power flow in branch l (line, link, or transformers) at time t
$\bar{g}_{n,s}$	Nominal power of generator, if extendable
$\bar{h}_{n,s}$	Nominal power of store, if extendable
F_l	Capacity of branch l, if extendable

b) Link constraints: Controllable links are restricted by the nominal capacity of the branch:

$$|f_{l,t}| \leq F_l \tag{5}$$

Links that are constrained by time-dependent restrictions:

$$\tilde{f}_{l,t} \cdot F_l \leq f_{l,t} \leq \bar{f}_{l,t} \cdot F_l \tag{6}$$

If the nominal power of the link is extendable in the optimization:

$$\tilde{f}_l \leq \bar{f}_l \leq \hat{f}_l \tag{7}$$

Links with ramping limits obey ramping constraints:

$$-rd_l \cdot F_l \leq (f_{l,t} - f_{l,t-1}) \leq ru_l \cdot F_l \quad \text{for } t \in \{1, \ldots, |T| - 1\}. \tag{8}$$

c) Store constraints: The store dispatch is not constrained within the store unit itself, as the store is connected to the network through links:

$$-\infty \leq h_{n,s,t} \leq +\infty \tag{9}$$

If the nominal power of the store is extendable in the optimization:

$$\tilde{e}_{n,s} \leq \bar{e}_{n,s} \leq \hat{e}_{n,s} \tag{10}$$

The dispatch of the store and the energy stored in the store unit are related by:

$$e_{n,s,t} = \eta_{\text{stand},n,s} \cdot e_{n,s,t-1} - h_{n,s,t} \tag{11}$$

The energy that is stored is subject to minimum and maximum fill levels of the store:

$$\tilde{e}_{n,s,t} \cdot \bar{e}_{n,s} \leq e_{n,s,t} \leq \bar{e}_{n,s,t} \cdot \bar{e}_{n,s} \tag{12}$$

In order to ensure that storage systems do not accumulate or deplete energy over the modeled time horizon, a cyclicity constraint is applied:

$$e_{n,s,t=-1} = e_{n,s,t=-T-1} \quad \text{for } t \in \{-1, \ldots, |T| - 1\} \tag{13}$$

d) Line and Transformer constraints: Similar to the links, the lines and the transformer are constrained to their nominal capacity of the branch:

$$|f_{l,t}| \leq F_l \tag{14}$$

Power flows in lines and transformers must comply to Kirchhoff's circuit laws. PyPSA uses the cycle-based formulation of KVL:

$$\sum_l C_{l,c} x_l f_{l,t} = 0 \quad \forall c \tag{15}$$

Where the cycle-based matrix C is constructed from the network graph, and x_l represents the series reactance.

e) Energy flow balances: The energy flow balance ensures that the energy flow is balanced at each bus n for each time t:

$$\sum_s g_{n,s,t} + \sum_s h_{n,s,t} - \sum_l K_{nl} f_{l,t} = \sum_s d_{n,s,t} \tag{16}$$

Where $d_{n,s,t}$ is the exogenous load at each node and K_{nl} is the incidence matrix for the network graph which indicates if a branch starts or ends at that node.

f) Custom constraints: In addition to the model's technical constraints, certain operational constraints are manually incorporated to capture specific system behavior.

1) *electrolyzers constraint:* ensures that the electrolyzers operate following the wind power generation profile of the IJmuiden Ver wind farm:

$$f_{l,t}^{\min,\text{pu,electrolyzer}} = f_{l,t}^{\max,\text{pu,electrolyzer}} =$$
$$\begin{cases} 1.0, & \text{if } g_{n,s,t-1}^{\text{windfarm IJV}} \geq f_l^{\max,\text{pu,electrolyzer}} \cdot \bar{F}_l^{\text{electrolyzer}}, \\ f_l^{\min,\text{pu,electrolyzer}}, & \text{if } g_{n,s,t-1}^{\text{windfarm IJV}} \leq f_l^{\min,\text{pu,electrolyzer}} \cdot \bar{F}_l^{\text{electrolyzer}}, \\ \dfrac{g_{n,s,t-1}^{\text{windfarm IJV}}}{\bar{F}_l^{\text{electrolyzer}}}, & \text{otherwise.} \end{cases}$$
$$\tag{17}$$

2) *Electricity load shedding constraint:*

$$-g_{n,s,t}^{\text{shed}} = \max\left(0,\ d_{n,s,t}^{\text{NL}} - \left[\sum_{s' \in S^{\text{elec}}} g_{n,s',t} + \sum_{s' \in S^{\text{elec}}} h_{n,s',t} \right.\right.$$
$$\left.\left. + \sum_{l' \in L^{\text{elec}}} K_{nl} f_{l',t} - \sum_{s' \in S^{\text{elec}}} d_{n,s',t}^{\text{Industry}}\right]\right), \quad \forall s \in S^{\text{elec}} \tag{18}$$

3) *Hydrogen load shedding:*

$$-g_{n,s,t}^{\text{shed}} = \max\left(0,\ d_{n,s,t}^{\text{H2 export}} - \left[\sum_{s' \in S^{\text{H2}}} g_{n,s',t} + \sum_{s' \in S^{\text{H2}}} h_{n,s',t} \right.\right.$$
$$\left.\left. + \sum_{l' \in L^{\text{H2}}} K_{nl} f_{l',t} - \sum_{s' \in S^{\text{H2}}} d_{n,s',t}^{\text{Industry}}\right]\right), \quad \forall s \in S^{\text{H2}} \tag{19}$$

D. Model Assumptions

To clarify the model's scope and limitations, the following key assumptions are made:

- Full collaboration among all stakeholders is assumed, including complete data transparency and a shared objective of minimizing total system costs.
- The model operates under perfect foresight, with complete knowledge of future system states.
- All energy carriers are assumed to function within centralized, regulated market structures.
- Fixed carrier price time series, not taking into account feedback mechanisms.

E. Power Flow Modeling

1) Electrical Power Flow modeling: PyPSA is selected as the modeling toolbox for this study due to its ability to represent power systems with high technical detail. This level of detail is essential to assess the technical feasibility in the electrical infrastructure. Power injections at each bus n are modeled and calculated using a linear approximation of the AC power flow equations:

$$P_n = \sum_m (KBK^T)_{nm}\theta_m - \sum_l K_{n\ell}b_\ell\theta_\ell^{\text{shift}} \quad (20)$$

Here, K is the network's incidence matrix, B represents the series susceptances, θ_n are the voltage angles, $\theta_\ell^{\text{shift}}$ are transformer phase-shifts.

2) Non-electrical Power Flow: Non-electrical networks are represented using the energy hub approach where energy flows and conversions are governed by fixed efficiency values rather than detailed physical models:

$$\begin{pmatrix} P_\alpha^{\text{out}} \\ P_\beta^{\text{out}} \\ \vdots \\ P_\omega^{\text{out}} \end{pmatrix} = \begin{pmatrix} \eta_{\alpha,\alpha} & \eta_{\beta,\alpha} & \cdots & \eta_{\omega,\alpha} \\ \eta_{\alpha,\beta} & \eta_{\beta,\beta} & \cdots & \eta_{\omega,\beta} \\ \vdots & \vdots & \ddots & \vdots \\ \eta_{\alpha,\omega} & \eta_{\beta,\omega} & \cdots & \eta_{\omega,\omega} \end{pmatrix} \begin{pmatrix} P_\alpha^{\text{in}} \\ P_\beta^{\text{in}} \\ \vdots \\ P_\omega^{\text{in}} \end{pmatrix}$$

In this formulation, each matrix element $\eta_{i,j}$ represents the efficiency of converting input from carrier j into output in carrier i. This approach enables scalable and integrated modeling of sector coupling, while still capturing key transformation losses and operational constraints in the optimization process.

F. Scenarios

To evaluate the impact of meteorological variability on system operation, a scenario-based analysis was performed using historical hourly wind speed and solar irradiance data from the KNMI station at Hoek van Holland (1970–2025). Scenario definition was based on wind availability, as the system is dominated by wind energy. Given the inverse correlation between wind speed and solar irradiance, years with opposing extremes were selected—such as a year with low wind and high solar for the worst-case, and high wind with low solar for the best-case. These time series were directly applied to define the renewable availability profiles in the model.

TABLE IV
KEY METEOROLOGICAL CHARACTERISTICS OF SCENARIOS.

Scenario	Average Annual Wind Speed	Average Annual Solar Irradiance
Worst-Case	5.49 m/s (1971)	143.77 W/m^2 (2022)
Normal-Case	6.81 m/s (2024)	123 W/m^2 (2024)
Best-Case	9.10 m/s (1992)	114.83 W/m^2 (2000)

G. Sensitivity Analysis

The sensitivity analysis conducted in this study employs stepwise deterministic sensitivity analysis (DSA). The sensitivity analysis examined five key variables: electricity export volume, hydrogen export volume, electricity market price, hydrogen market price, and ammonia market price. For each variable, the analysis tested variations ranging from -50% below to +50% above the baseline value, in increments of 10%, while all other input parameters are held constant at normal-case levels.

IV. RESULTS AND DISCUSSION

This section evaluates the performance of the MES under varying scenarios and proposes a novel operation strategy suited for future multi-energy system integrating natural gas, electricity, hydrogen, ammonia, and heat. The analysis is conducted across three main areas: system behavior under the normal-case scenario, scenario comparisons, and the formulation of a new system operation strategy.

1) Normal-Case Scenario Analysis:

a) Electricity Network: The electricity system demonstrates strong reliance on offshore wind generation with notable curtailment, suggesting potential for additional hydrogen production through electrolysis. Battery storage provides stabilization against price fluctuations and reliability support during low renewable generation. Ammonia-fired power plants are prioritized over hydrogen-fired plants during periods of low wind generation, despite higher fuel costs, due to ammonia's abundance, direct use capability for power generation, and lower fixed operational costs of power plant operation. In periods of low wind, the system dynamically responds by down-scaling ATR to reduce its electricity consumption, discharging batteries, and activating hydrogen-fired generation. This highlights the effectiveness of dynamic MES operation based on resource availability. An example of a system response to electricity scarcity is illustrated in Figure 2, while the corresponding behavior in the hydrogen network is shown in Figure 3.

b) Hydrogen Network: Hydrogen is the primary enabler for industrial decarbonization by replacing natural gas in high-temperature processes. Multiple hydrogen sources supply the system's demand: 14% from imports (10% LH2, 4% LOHC), 19% from autothermal reforming, 21% from electrolyzers, and 46% from ammonia cracking. Hydrogen production from electrolyzer is dependent on wind generation. Hydrogen storage systems balance supply during reduced production periods. Hydrogen tank storage supplements underground storage when injection/production limits due to pressure constraints
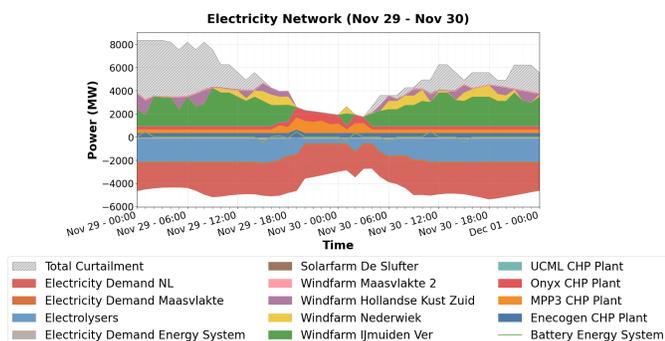
Fig. 2. Electrical power dispatch and demand for November 29-30. Onyx and MPP3 CHP plants are ammonia-fired. Enecogen and UCML CHP plants are hydrogen-fired.

Fig. 4. Charging/discharging power and stored energy of ammonia storage.

are reached. Variable hydrogen production and demand are dynamically balanced. Figure 3 illustrates how, at the same moment as electricity scarcity occurs (see Figure 2), hydrogen availability also declines due to reduced electrolyzer output and occasional ATR down-scaling. The figure shows how the system responds by activating hydrogen storage and increasing ammonia cracking to maintain supply.
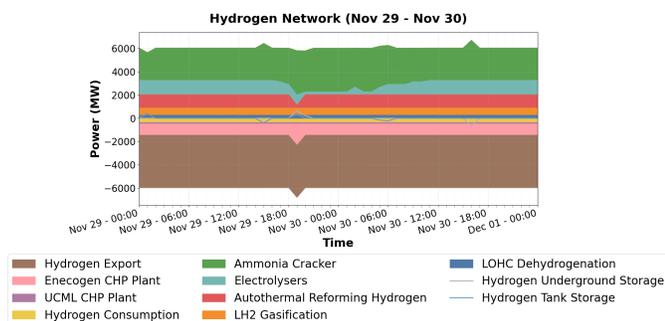

Fig. 3. Hydrogen power dispatch and demand for Nov 29-30.

c) Ammonia Network: Ammonia emerges as the primary flexibility provider. The system distributes ammonia through hydrogen production, electricity generation, storage management, and export, based on system's needs. Ammonia storage supplies large volumes to power plants during low wind generation periods. This behavior is illustrated in Figure 4, which shows ammonia is primarily accumulated and then discharged in concentrated periods—corresponding to times of reduced wind availability. Ammonia's flexibility stems from wind-independence, variable export capacity, connections to both electricity and hydrogen networks, and cost-effectiveness for large-scale storage.

d) Natural Gas Network: Natural gas is imported at a constant rate via the LNG terminal, mainly for export, with a small share used in the ATR process. The ATR plant operates at full capacity due to low marginal costs but reduces output during electricity scarcity to conserve power. Fixed carrier prices are assumed, so market effects of ATR curtailment are not captured—potentially underestimating the value of continuous ATR operation. A refinement could involve keeping ATR
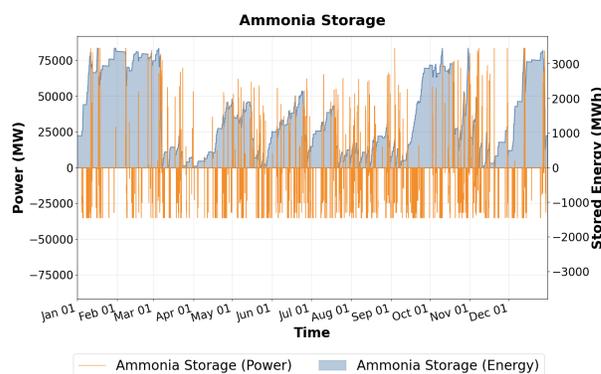
output constant while applying flexibility through targeted DR or DSM programs to stabilize hydrogen prices.

e) Heat Network: The heat network mainly delivers residual industrial heat (at 70°C / 120°C) to the WarmtelinQ district heating network, offering a constant baseline supply. However, due to the higher heat needs (ca. 400°C) of local industry, the network primarily improves overall energy efficiency rather than enhancing system flexibility.

A. Scenario Comparison

Three scenarios—worst-case, normal-case, and best-case—were developed to assess system performance under varying wind conditions. Increased wind availability reduces the frequency and duration of windless periods, but even in the best-case, brief shortages persist, requiring flexibility solutions. Storage requirements shift significantly across

TABLE V
SCENARIO RESULT COMPARISON.

	Worst-Case	Normal-Case	Best-Case
Wind Resource Availability	Low	Medium	High
Frequency of windless hours	20.50%	7.55%	0.46%
Average duration of a windless period	5.15 h	3.98 h	2.39 h
Hydrogen Underground Storage Capacity	1477 MWh	898 MWh	667 MWh
Hydrogen Tank Storage Capacity	201 MWh	397 MWh	865 MWh
Ammonia Storage Capacity	311814 MWh	83459 MWh	11372 MWh
Battery Storage Capacity	932 MWh	467 MWh	213 MWh
Operation > min. Load - Ammonia CHP Plants	28.67%	14.01%	2.91%
Operation > min. Load - Hydrogen CHP Plants	0.28%	0.24%	0.11%
Renewable Electricity Curtailment	38.79 %	44.82%	53.01%
Load Schedding - Electricity	0 MW	0 MW	0 MW
Load Schedding - Hydrogen	0 MW	0 MW	0 MW
Total System Cost (Investment + Operation)	34.1 bln Euro	34.0 bln Euro	33.4 bln Euro

scenarios. As wind conditions improve, needs for battery, ammonia, and underground hydrogen storage decrease, reflecting fewer and shorter renewable shortfalls. Conversely, hydrogen tank storage increases, as it offers a cost-effective backup for rare shortages compared to underutilized batteries. Ammonia-fired power plant operation drops sharply (-89.9% worst- to best-case), while hydrogen-fired plants decrease more modestly (-60.7%), highlighting the shift toward hydrogen storage for short-term balancing.

The increased storage capacity observed in the worst-case scenario suggests that to ensure operational robustness, reserve storage capacities should be considered. Such additional capacity enables the system's operation to remain stable and resilient across a broad range of weather scenarios.

B. Sensitivity Analysis

The sensitivity analysis examines how export volumes and energy carrier prices impact system operation under uncertainty. Export volumes significantly affect storage capacity and CHP operations, with all storage requirements increasing with rising export demand. These volume changes have relatively small effects on total system costs. Reducing export volumes could decrease required storage capacities, particularly of interest for spatially-constrained ammonia storage.

In contrast, carrier price variations (hydrogen, electricity, ammonia) minimally affect total storage capacity and CHP operation but substantially impact total system costs by influencing marginal costs throughout the system.

Price variations shift the relative use of storage types rather than causing uniform scaling. Low electricity prices favor underground hydrogen storage, while high prices increase reliance on batteries. Ammonia price changes influence the trade-off between hydrogen tank storage and batteries, with low ammonia prices favoring hydrogen-fired power generation and hydrogen tank storage for electricity balancing. Hydrogen price effects are similar but less pronounced, with low prices promoting hydrogen tank storage and hydrogen-fired power generation, and high prices increasing battery use. These results underscore the importance of accounting for export assumptions and price volatility when designing flexible multi-energy systems.

C. System Operation Strategy

A novel operation strategy for the MES was developed, derived from the system's optimal operation. The strategy moves beyond conventional, uni-sectoral, static and price-driven dispatch by integrating dynamic dispatch response, multi-carrier coordination, and operational flexibility, while ensuring industrial energy reliability. Four core principles underpin this strategy: (1) cross-sector economic optimization, (2) dynamic responsiveness to system states, (3) multifunctional carrier flexibility (notably hydrogen and ammonia), and (4) uninterrupted supply to local industry.

Electricity from VRES is prioritized; during shortages, ammonia-fired plants ramp up first, followed by hydrogen-fired plants or battery discharge based on system conditions. Hydrogen supply is stabilized via dynamic and coordinated operation of ATR, electrolyzers, ammonia cracking, and hydrogen storages. Wind energy is directed to electrolyzers to reduce grid congestion.

a) Strategic Implications: The strategy demonstrates that a MES operation, leveraging multifunctional energy carriers and dynamic coordination, greatly enhances flexibility and resilience in renewable-dominated energy systems. Ammonia emerges as the central enabler due to its non-intermittent nature, cost-effective storage, and cross-sector connectivity. Storage play a key role in balancing and storage technologies must be tailored to both duration and frequency of balancing needs. This framework provides a robust foundation for future MES operation, emphasizing adaptability, cost-efficiency, and secure supply across all energy carriers.

V. CONCLUSION AND FUTURE RESEARCH

This research has developed a novel model-based approach for optimizing integrated multi-energy systems, including an operation strategy that fundamentally prioritizes cross-sector economic optimization, dynamic dispatch response, enhanced system flexibility, and industrial supply reliability. Numerical simulations conducted on a test system identify ammonia as a critical flexibility provider due to its wind-independent import capabilities, cost-effective storage potential, and ability to stabilize both hydrogen and electricity networks. Strategic integration of storage and conversion technologies enables effective management of renewable intermittency while ensuring reliable energy supply. Future work should focus on incorporating more detailed physical models of energy carrier networks and implementing finer temporal resolutions to capture short-term dynamics and component response times.

REFERENCES

[1] P. Mancerella, "MES (multi-energy systems): An overview of concepts and evaluation models," in Energy, vol. 65, February 2014.
[2] L. Kriechbaum, G. Scheiber, T. Kienberger , "Grid-based multi-energy systems—modelling, assessment, open source modelling frameworks and challenges," in Energy, Sustainability and Society 8, November 2018.
[3] P. Gabrielli, M. Gazzani, E. Martelli, M. Mazzotti, "Optimal design of multi-energy systems with seasonal storage," in Applied Energy, vol. 219, pp. 408–424, June 2018.
[4] Q. Zhang, J. Qi, L. Zhen, "Optimization of integrated energy system considering multi-energy collaboration in carbon-free hydrogen port," in Transportation Research Part E: Logistics and Transportation Review, vol. 180, December 2023.
[5] D. Yang, M. Wang, "Optimal operation of an integrated energy system by considering the multi energy coupling, AC-DC topology and demand responses," in International Journal of Electrical Power & Energy Systems, vol. 129, July 2021.
[6] O. Siddiqui, I. Dincer, "Design and analysis of a novel solar-wind based integrated energy system utilizing ammonia for energy storage," Energy Conversion and Management, vol. 195, pp. 866-884, September 2019.
[7] J. Zhou, Z. Zhang, R. Zhang, W. Zhang, G. Xu, H. Wang, "Optimal capacity and multi-stable flexible operation strategy of green ammonia systems: Adapting to fluctuations in renewable energy", vol. 314, August 2024.
[8] S. Yang, H. Wu, J. Song, H. Li, H. Chen, "Two-stage robust optimization scheduling for integrated energy systems considering ammonia energy and waste heat utilization", in Energy Conversion and Management, vol. 319, November 2024.
[9] B. Koirala, S. Hers, G. Morales-España, Ö. Özdemir, J. Sijm, M. Weeda, "Integrated electricity, hydrogen and methane system modelling framework: Application to the Dutch Infrastructure Outlook 2050", in Applied Energy, vol. 289, May 2021.
[10] D. Wen, M. Aziz, "Flexible operation strategy of an integrated renewable multi-generation system for electricity, hydrogen, ammonia, and heating", in Energy Conversion and Management, vol. 253, February 2022.
[11] Y. Wang, C. Shao, "Optimal Operation Model of the Multi-Energy Network in the Distribution System," in 2019 IEEE International Conference on Energy Internet (ICEI), May 2019.
[12] T. Brown, J. Hörsch, D. Schlachtberger, "PyPSA: Python for Power System Analysis," in Journal of Open Research Software, vol. 6, January 2018.